NORPIE/98
Nordic Workshop on Power and Industrial Electronics
Espoo, Finland, August 26–27, 1998

VIENNA Rectifier III – A Novel Three-Phase Single-Stage Buck-Derived Unity Power Factor AC-to-DC Converter System

Johann W. Kolar, Uwe Drofenik, Hans Ertl*, Franz C. Zach*
Technical University Vienna
Dept. of Electrical Machines and Drives 372
Dept. of Applied Electronics 359.5
Gusshausstr. 27, A-1040 Wien, AUSTRIA
Tel.: +43-1-58801-3916, Fax.: +43-1-5036176
email: hkolar@ieam.tuwien.ac.at

Abstract – In the area of AC/DC converters with low effects on the mains single-stage rectifier systems gain more and more importance. The basic characteristic of these systems is the direct integration of a high-frequency isolation of the output circuit into the converter topology. This makes possible the matching of the output and mains voltage levels besides the sinusoidal guidance of the mains currents and a highly dynamic control of the output voltage. Also, higher efficiency and a lower realization effort as compared to a two-stage, i.e., AC/DC-DC/DC engergy conversion results. In this paper the topology of a novel single-stage three-phase PWM rectifier system with impressed output current is developed starting from a two-stage converter concept. After the description of the basic function of the circuit (called *VIENNA Rectifier III*) the conduction states and the current space vectors available for forming the input currents are determined; a simple multi-loop control of the converter is proposed which also guarantees a symmetric transformer magnetization based on pre-control signals. Furthermore, the theoretical considerations are verified by digital simulation and the current stresses on the power semiconductor devices are calculated in analytically closed form. Finally, a short preview on the planned continuation of the research is given.

1 Introduction

In [1] a quasi-single-stage three-phase AC/DC converter has been proposed (cf. **Fig.1**(a)) which yields a reduction of the realization effort of a conventional dual-stage buck-type PWM rectifier system. A basic disadvantage of this converter (analyzed in detail in [2]) consists, however, in the combination of a bidirectional input stage (which would also allow energy feed-back into the mains) with an output stage which is capable only for rectification. If, based on this consideration, the input stage is replaced by

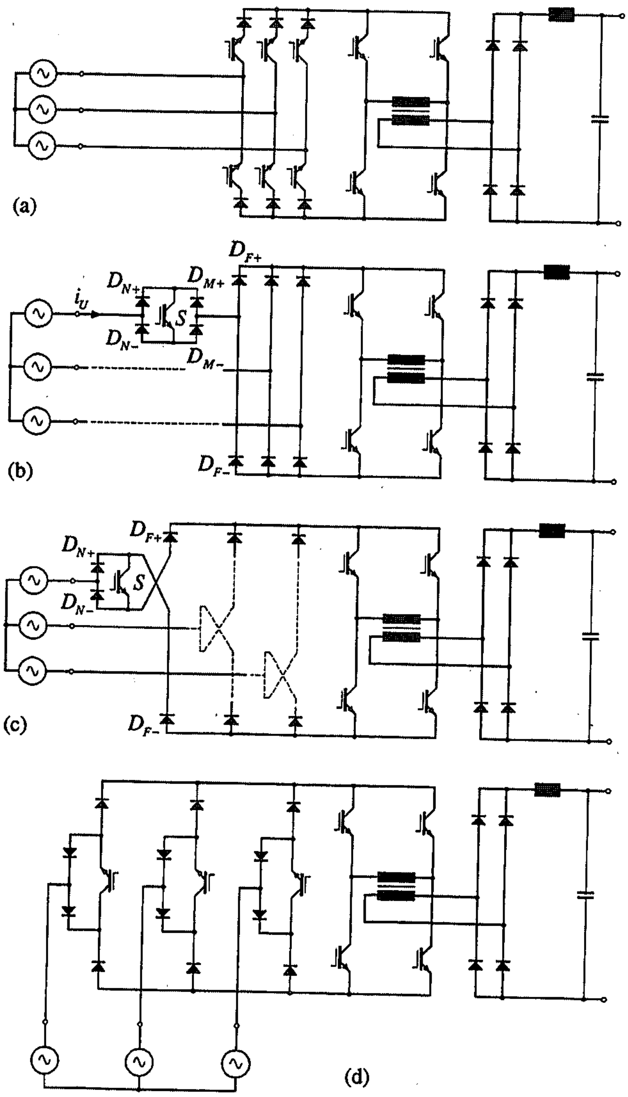

Fig.1: Derivation of the circuit structure of a novel single-stage three-phase buck-type PWM rectifier system **(f)** starting from the

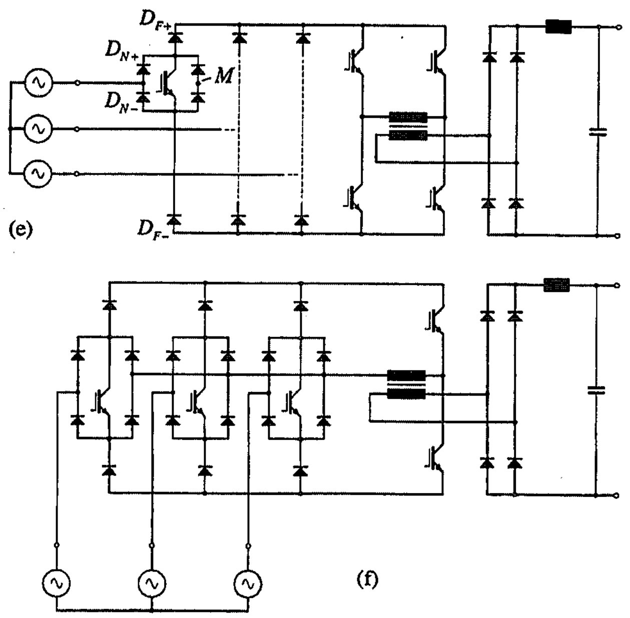

quasi single-stage topology (a) proposed in [1]. For practical realization the impressed input voltages of the system (represented by voltage sources) are realized by a star- or delta-connection of filtering capacitors (cf. Fig.2).

a unidirectional circuit as proposed in [3], or if the system operation is limited to resistive (ohmic) mains behavior, the converter topology shown in Fig.1(b) results. There, a possibility of a further simplification of the circuit structure and a reduction of the conduction losses is given by the fact that a positive input phase current $i_U > 0$ is flowing via D_{N+} and S, and the series connection D_{M-}, D_{F+} and a negative input phase current $i_U < 0$ is fed through D_{N-}, S, and D_{M+}, D_{F-}. Therefore, the diodes D_{M-} and D_{M+} can be omitted (cf. Fig.1(c) and/or Fig.1(d), and/or Fig.3 in [4]).

With the aim to minimize the number of turn-off power semiconductors one should consider alternatively, however, with respect to Fig.3 of [5], an integration of the 4-quadrant switching elements (i.e., the combination of D_{N+}, D_{N-}, D_{M-}, D_{M+} and S) of the phases into the bridge legs D_{F+}, D_{F-} of the input diode bridge [6] (cf. Abb.1(e)). Although this leads to the loss of the controllability of the current flowing through the diodes $D_{F+,i}$ and $D_{F-,i}$ of each phase i, this modification gives for each phase a switching node M which can be connected with the input via the power transistor S_i. Therefore, in analogy to [5], the possibility to transferring the function of a bridge leg of the DC/DC converter stage to the input stage is given. The resulting novel circuit topology of a single-stage three-phase buck-type PWM rectifier system having only 5 turn-off power semiconductor devices is shown in Fig.1(f) and **Fig.2**, respectively.

As the following considerations will show, this system based on a step-down converter makes possible

- a sinusoidal control of the mains currents in phase with the related phase voltages,
- a highly dynamic control of the output current and/or of the output voltage and
- the limitation of the input current in case of a short circuit of the output voltage and/or for a direct start-up without previous pre-charging of the output capacitor.

Therefore, the proposed system is ideally suited for, e.g., the realization of welding current sources with low effects on the mains or for telecom power supply modules with high efficiency and high power density, respectively.

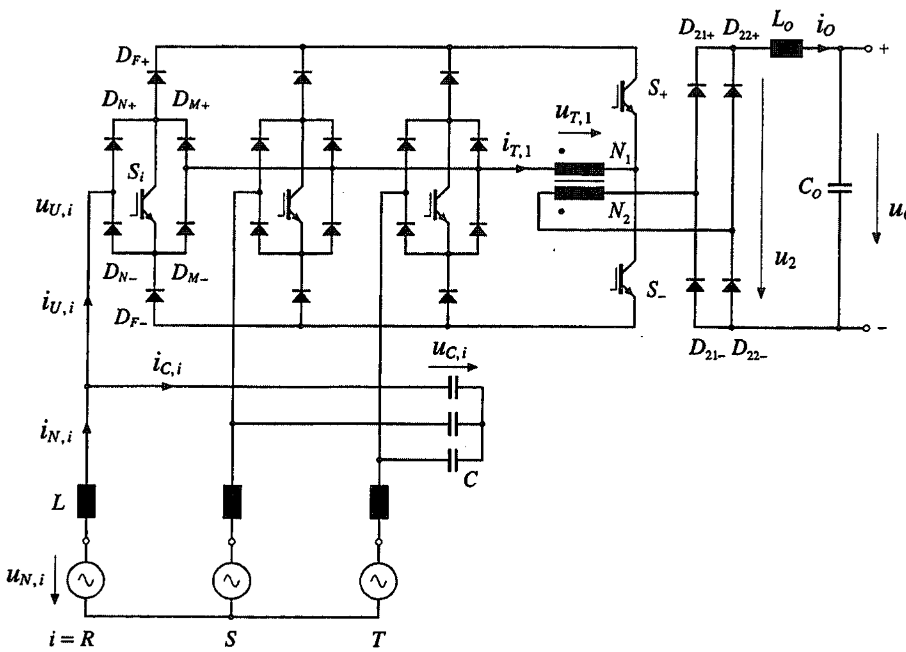

Fig.2: Basic structure of the power circuit of the proposed novel three-phase PWM rectifier with integrated isolation and impressed output current. Besides the given derivation, the system can also be thought to be formed by a dual exchange of the input and output side energy storage elements of a VIENNA Rectifier II (cf. [5]). Accordingly, the system proposed in this paper will be called *VIENNA Rectifier III*. The supplying three-phase mains is represented by ideal voltage sources $u_{N,i}$, $i = R, S, T$.

2 Analysis of the Basic Function of the System

An ideally sinusoidal shape

$$\underline{i}_{N,(1)} = \hat{I}_{N,(1)} \exp j\varphi_N \qquad (1)$$

of the mains current, aligned in phase with the mains voltage

$$\underline{u}_N = \hat{U}_N \exp j\varphi_N \,, \qquad (2)$$

would be obtained for purely sinusoidal current consumption

$$\underline{i}_U^* = \underline{i}_{N,(1)} - j\frac{1}{\omega_N C}\underline{u}_N \qquad \omega_N = 2\pi f_N \qquad (3)$$

of the rectifier system. There, the quantities $\underline{i}_{N,(1)}$, $\underline{u}_N$ und $\underline{i}_U^*$ denote the complex space vectors related to the phase quantities $i_{N,i}$, $u_{N,i}$ and $i_{U,i}^*$, $i = R, S, T$.

Remark: The space vector is calculated based on the triple of phase quantities

$$\begin{aligned} u_{N,R} &= \hat{U}_N \cos\varphi_N \\ u_{N,S} &= \hat{U}_N \cos(\varphi_N - \frac{2\pi}{3}) \\ u_{N,T} &= \hat{U}_N \cos(\varphi_N + \frac{2\pi}{3}) \end{aligned} \qquad (4)$$

with

$$\varphi_N = \omega_N t \qquad (5)$$

according to the defining equation

$$\underline{u}_N = \frac{2}{3}(u_{N,R} + \underline{a}u_{N,S} + \underline{a}^2 u_{N,T}) \qquad \underline{a} = \exp j\frac{2\pi}{3} \qquad (6)$$

(shown for the mains voltage).

In reality, $\underline{i}_U^*$ can only be formed as fundamental component $\underline{i}_{U,(1)}$ of the discontinuous rectifier input phase currents $i_{U,i}$ (the switching frequency components are largely suppressed by the LC input filter). The derivation of an appropriate control method is the aim of the following considerations. For the sake of simplicity and for the purpose of a limitation to the essentials we there will assume

- a purely sinusoidal shape (identical to the mains voltage) of the capacitor voltage $u_{C,i} \approx u_{N,i}$, i.e., the voltage drop at mains frequency $j\omega_N L\hat{I}_{N,(1)} \approx 0.005\ldots 0.01\hat{U}_N$ across the series inductances L are neglected, as well as the ripple of the capacitor voltages,
- a mains current approximately equal to the fundamental of the rectifier input current ($i_{N,i} \approx i_{N,(1),i} \approx i_{U,(1),i}$), i.e., the mains current ripple and the reactive current due to the filtering capacitors C are neglected. Furthermore,
- the magnetizing current i_m and the leakage of the transformer will be neglected, and
- a constant output current $i_O = I_O$

will be assumed. Despite these neglections, the real conditions for high pulse frequencies are closely approximated.

2.1 Conduction States and Current Space Vectors

The basis of the derivation of a concept for controlling the mains current is the knowledge of the admissible switching states and/or of the related conduction states (cf. **Fig.3**) of

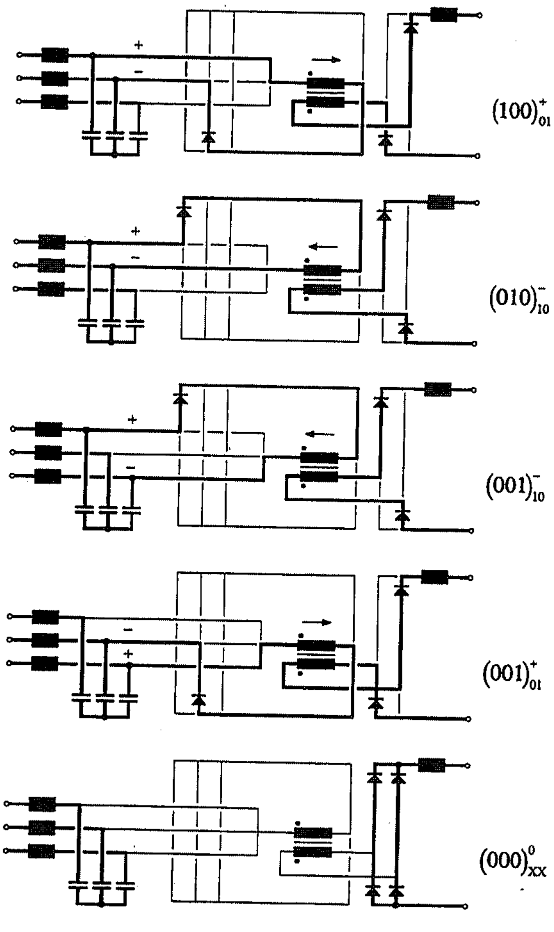

Fig.3: Possible conduction states of the rectifier system within $\varphi_N \in (-\frac{\pi}{3}, 0)$ and/or for $u_{N,R} \geq u_{N,T} \geq u_{N,S}$ or $u_{N,RS} > 0, u_{N,ST} < 0$ and $u_{N,TR} < 0$. For the sake of clearness, the connection of the switching elements S_R, S_S and S_T with the transformer primary N_1 are shown for each phase separately. (This deviates from the circuit structure shown in Fig.1.) For $s_R = s_S = s_T = 0$ there results (independently of s_+ and s_-) a freewheeling state of the output current via the diode bridge on the secondary; there exists no current flow via the primary and no rectifier input current $i_{U,i}$. For s_+ and s_- one sets $s_+ = s_- = $ x accordingly. (By $s_+ s_- = 10$ or 01 or 00 only the guidance of the transformer magnetizing current is influenced which is not treated in detail here.)

s_R	s_S	s_T	s_+	s_-	$i_{U,R}$	$i_{U,S}$	$i_{U,T}$	$\underline{i}_{U,j}$	$u_{T,1}$	sign$(u_{T,1})$
0	0	0	x	x	0	0	0	0	0	0
0	0	1	0	1	0	$-\frac{N_2}{N_1}I_O$	$+\frac{N_2}{N_1}I_O$	$\frac{2}{\sqrt{3}}\frac{N_2}{N_1}I_O\exp(-j\frac{\pi}{2})$	$-u_{N,ST}$	+
0	0	1	1	0	$+\frac{N_2}{N_1}I_O$	0	$-\frac{N_2}{N_1}I_O$	$\frac{2}{\sqrt{3}}\frac{N_2}{N_1}I_O\exp(+j\frac{\pi}{6})$	$-u_{N,RT}$	−
0	1	0	1	0	$+\frac{N_2}{N_1}I_O$	$-\frac{N_2}{N_1}I_O$	0	$\frac{2}{\sqrt{3}}\frac{N_2}{N_1}I_O\exp(-j\frac{\pi}{6})$	$-u_{N,RS}$	−
1	0	0	0	1	$+\frac{N_2}{N_1}I_O$	$-\frac{N_2}{N_1}I_O$	0	$\frac{2}{\sqrt{3}}\frac{N_2}{N_1}I_O\exp(-j\frac{\pi}{6})$	$+u_{N,RS}$	+

Tab.1: Admissible switching states s_R, s_S and s_T of the rectifier system and related switching states s_+ and s_- as well as the rectifier input phase currents $i_{U,i}$, rectifier input current space vectors $\underline{i}_{U,j}$, transformer primary voltages $u_{T,1}$ and signs sign$(u_{T,1})$ for $\varphi_N \in (-\frac{\pi}{3}, 0)$ and/or $u_{N,RS} > 0$ and $u_{N,ST}, u_{N,TR} < 0$; for $u_{T,1} = 0$ we set sign$(u_{T,1})$=0.

the system which can be denoted in accordance to [5] by the combination

$$j = (s_R s_S s_T)_{s_+ s_-}^{\mathrm{sign}(u_{T,1})} \tag{7}$$

of the switching functions s_R, s_S, s_T, s_+ and s_- of the power transistors S_R, S_S, S_T, S_+ and S_-. There, $s_i = 1$ denotes the on-state and $s_i = 0$ the off-state of a valve. Sign$(u_{T,1})$ gives the direction of the voltage $u_{T,1}$ across the primary winding N_1 of the transformer.

In order to avoid a short circuit of a line-to-line voltage, always only one of the bidirectional bipolar switches S_i, $i = R, S, T$ and only one of the power transistorsr S_+, S_- may be turned on. Furthermore, also all valves S_R, S_S and S_T may remain in the off-state. The thereby possible switching states j of the rectifier system are compiled in **Tab.1**.

As is evident immediately, the conduction states related to the switching states j are determined by the signs and the magnitude ratio of the line-to-line capacitor and/or mains voltages

$$u_{N,RS} = \sqrt{3}\hat{U}_N \cos(\varphi_N + \frac{\pi}{6}) \tag{8}$$
$$u_{N,ST} = \sqrt{3}\hat{U}_N \sin(\varphi_N) \tag{9}$$
$$u_{N,TR} = -\sqrt{3}\hat{U}_N \cos(\varphi_N - \frac{\pi}{6})\,. \tag{10}$$

By considering the phase symmetry of the converter structure and the symmetries of the assumed purely sinusoidal mains voltage system (cf. Eq.(4)) a detailed analysis can be constrained to a $\frac{\pi}{3}$-wide interval of the mains period. In the case at hand the interval $\varphi_N \in (-\frac{\pi}{3}, 0)$ is considered and/or $u_{N,RS} > 0$, $u_{N,ST} < 0$, $u_{N,TR} < 0$ is assumed.

For $j = (100)_{01}^{+}$ the line-to-line voltage $u_{N,RS}$ is being impressed in the direction $u_{T,1}$ (sign$(u_{T,1}) = +$) across the transformer primary. The output current I_O is conducted accordingly via the diodes D_{22+} and D_{21-}. According to the balance of primary and secondary ampere windings a current $i_{T,1} = i_{U,R} = -i_{U,S} = \frac{N_2}{N_1}I_O$ results on the primary (cf. Tab.1). For $j = (010)_{10}^{-}$ the mains-side conditions and the magnitude of the transformer primary voltage remain unchanged. However, now sign$(u_{T,1}) = -$ is valid. Related to the forming of the input phase currents $j = (100)_{01}^{+}$ and $j = (010)_{10}^{-}$ represent redundant switching states leading to, however, an opposite variation of the transformer magnetization. Especially clear representations of the conditions result for considering the space vectors $\underline{i}_{U,j}$ related to the phase quantities $i_{U,i,j}$ (cf. **Fig.4**). There, j again denotes the relevant switching state.

2.2 Control of the Input Current

For realization of a given reference value $\underline{i}_U^*$ of the input current and/or of a related mains current $\underline{i}_N \approx \underline{i}_U^*$ we have to apply the vectors $\underline{i}_{U,j}$ immediately neighbouring to $\underline{i}_U^*$ in order to achieve a deviation as small as possible between reference annd actual space vectors. There, the sequency

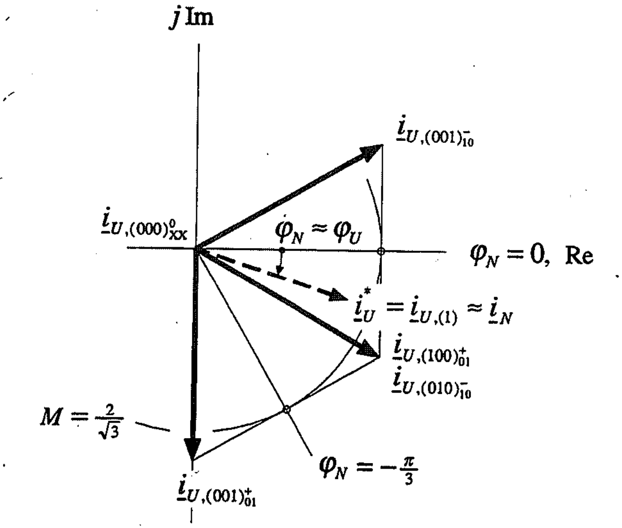

Fig.4: Space vectors $\underline{i}_{U,j}$ of the input phase currents $i_{U,i}$ related to the conduction states according to Fig.3; besides the respective switching state of the converter the index j also informs about the polarity sign$(u_{T,1})$ of the transformer primary voltage $u_{T,1}$. The switching states $(100)_{01}^{+}$ and $(010)_{10}^{-}$ are redundant with respect to the current generation; however, they lead to an opposite change of the magnetizing current i_m of the transformer.

of the switching states j forming the vectors $\underline{i}_{U,j}$ has to be selected within each pulse half period $\frac{1}{2}T_P$ in such a way that a minimum number of switching transitions of the power transistors lead to the next following switching state.

In $\varphi_N \in (-\frac{\pi}{6}, 0)$ and/or for $u_{N,RS} > 0$, $u_{N,TR} < u_{N,ST} < 0$ this is achieved by

$$\begin{gathered}\ldots|_{t_\mu=0}(100)^+_{01} - (000)^0_{xx} - (001)^-_{10} - (010)^-_{10}|_{t_\mu=\frac{1}{2}T_P} \\ (010)^-_{10} - (001)^-_{10} - (000)^0_{xx} - (100)^+_{01}|_{t_\mu=T_P}\ldots\end{gathered} \tag{11}$$

For the relative on-time of the switching states there follows via simple geometric considerations

$$\begin{aligned}\delta_{(001)^-_{10}} &= \frac{\sqrt{3}}{2}M\cos(\varphi_N - \frac{\pi}{3}) \\ \delta_{(100)^+_{01}} + \delta_{(010)^-_{10}} &= \frac{\sqrt{3}}{2}M\cos(\varphi_N + \frac{\pi}{3}) \\ \delta_{(000)^0_{xx}} &= 1 - \frac{\sqrt{3}}{2}M\cos(\varphi_N),\end{aligned} \tag{12}$$

where

$$M = \frac{\hat{I}_{U,(1)}}{\frac{\sqrt{3}}{2}\frac{N_2}{N_1}I_O} \tag{13}$$

denotes the modulation index of the pulse width modulation. Its definition has been selected such that, e.g., the range $M \in [0, \frac{2}{\sqrt{3}}]$ as known from the conventional DC voltage link PWM rectifier system is given.

Remark: For given input and output voltage the selection of M defines the turns ratio of the transformer. For neglecting the losses there follows from the input/output power balance of the system

$$\frac{3}{2}\hat{U}_N\hat{I}_N = U_O I_O \tag{14}$$

by consideration of Eq.(13)

$$\frac{N_1}{N_2} \approx \frac{3\sqrt{3}}{4}M\frac{\hat{U}_N}{U_O} \tag{15}$$

and/or with $M \leq \frac{2}{\sqrt{3}}$ there is given a maximum admissible value

$$\frac{N_1}{N_2} \leq \frac{3}{2}\frac{\hat{U}_N}{U_O} \tag{16}$$

of the transformation ratio.

2.3 Symmetrization of the Transformer Magnetization by Pre-Control Signals

By the requirement of a defined shape $\underline{i}^*_U$ of the local average value of the input current (i.e., the average value related to a pulse half period) only the relative *total* on-time of the redundant switching states $(100)^+_{01}$ and $(010)^-_{10}$ (cf. Eq.(12)) is defined. The distribution of this total on-time to the redundant switching states gives a degree of freedom of the system control which can be used for guaranteeing a purely AC magnetization of the transformer.

For this, the partition of the total on-time $\delta_{(100)^+_{01}} + \delta_{(010)^-_{10}}$ has to be performed such that the voltage-time area across the transformer within a pulse half period results to 0,

$$u_{T,1,\text{avg}} = \int_0^{\frac{1}{2}T_P} u_{T,1}\mathrm{d}t_\mu = 0\,, \tag{17}$$

this means that in the interval $\varphi_N \in (-\frac{\pi}{6}, 0)$ considered here we have

$$u_{N,RS}\,\delta_{(100)^+_{01}} = u_{N,RS}\,\delta_{(010)^-_{10}} + u_{N,RT}\,\delta_{(001)^-_{10}}\,. \tag{18}$$

Then, under consideration of Eq.(12) there follows

$$\frac{\delta_{(010)^-_{10}}}{\delta_{(100)^+_{01}} + \delta_{(010)^-_{10}}} = \frac{\sin(2\varphi_N)}{\sin(2\varphi_N) - \frac{\sqrt{3}}{2}}\,. \tag{19}$$

This distribution can be achieved for generation of the switching instants of the power transistors from intersections of the output signals of the capacitor phase voltage controllers $H(s)$ with a triangular pulse frequency carrier signal i_D being equal for all three phases (*ramp comparison control*, cf. [5]) by pre-control signals

$$\begin{aligned}\frac{1}{\hat{I}_D}m_{RS} &= 1 - \frac{3}{2}M\frac{\sin(\varphi_N - \frac{\pi}{6})}{\sin(2\varphi_N) - \frac{\sqrt{3}}{2}} \\ \frac{1}{\hat{I}_D}m_{ST} &= -1 + \sqrt{3}M\frac{\sin(2\varphi_N)\cos(\varphi_N + \frac{\pi}{3})}{\sin(2\varphi_N) - \frac{\sqrt{3}}{2}}\end{aligned}$$

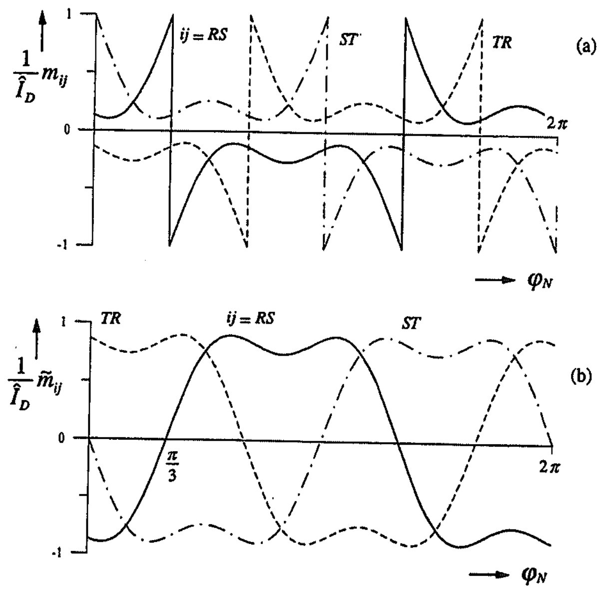

Fig.5: Shape of the pre-control signales m_{ij} of the ramp comparison control within a mains period (cf. **(a)**) rated with respect to $\hat{I}_D$. The continuous shape $\tilde{m}_{ij}$ of the pre-control signals as shown in **(b)** can be obtained based on (a) by addition of rectangular signals according to Eq.(21).

$$\frac{1}{\hat{I}_D} m_{TR} = -1 - \frac{\sqrt{3}}{2} M \frac{\sqrt{3}\sin(\varphi_N + \frac{\pi}{6})}{\sin(2\varphi_N) - \frac{\sqrt{3}}{2}} + \frac{\sqrt{3}}{2} M \frac{4\sin(\varphi_N)\cos^2(\varphi_N)}{\sin(2\varphi_N) - \frac{\sqrt{3}}{2}} \quad (20)$$

(cf. **Fig.5**(a)) valid in the angle interval $\varphi_N \in (-\frac{\pi}{6}, 0)$. There, a fundamental of the rectifier input current is set with the magnitude of the mains current reference value and/or the value of M (cf. Eq.(13)). The auxiliary switching functions s'_R, s'_S and s'_T (cf. **Fig.6**), resulting from the intersection, are then to be translated to get the actual control commands s_R, s_S, s_T according to **Tab.2**)

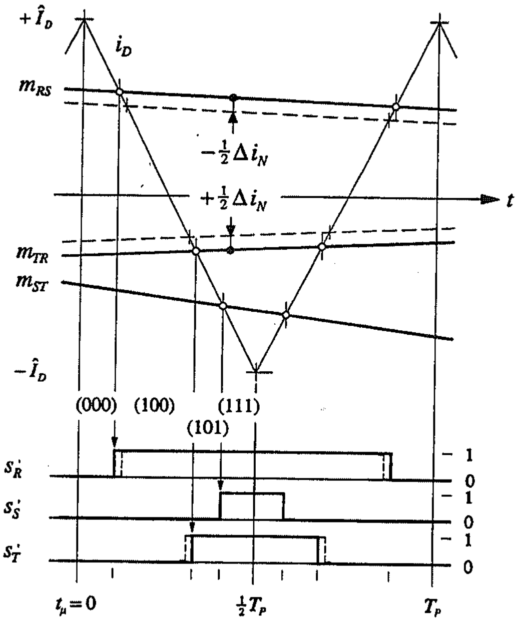

Fig.6: Time behavior of the triangular signal i_D, of the pre-control signals m_{ij} and of the auxiliary switching functions s'_i within one pulse period for $\varphi_N \in (-\frac{\pi}{6}, 0)$. According to Tab.2, the auxiliary switching function sequence $(s'_R s'_S s'_T)$ = (000) - (100) - (001) -(111) is coded into the sequence $j = (100)^+_{01}$ - $(000)^0_{xx}$ - $(001)^-_{10}$ - $(010)^-_{10}$ (cf. Eq.(11)). In order to achieve a current variation of, e.g., $\Delta i^*_{U,R} = +\Delta i_U$, $\Delta i^*_{U,S} = \Delta i^*_{U,T} = -\frac{1}{2}\Delta i_U$, the related line-to-line current variations $\Delta i^*_{U,RS} = +\frac{1}{2}\Delta i_U$, $\Delta i^*_{U,ST} = 0$, $\Delta i^*_{U,TR} = -\frac{1}{2}\Delta i_U$ (cf. Eq.(24)) have to be subtracted from the related pre-control signals. Thereby, the on-time of the switching states $j = (100)^+_{01}$ and $(001)^-_{10}$ is increased and/or according to Tab.1 $i_{U,R}$ is increased and $i_{U,S}$ and $i_{U,T}$ are decreased as required.

A continuous shape of the pre-control signals is achieved for

$$\tilde{m}_{ij} = \begin{cases} m_{ij} - \hat{I}_D & \text{for } m_{ij} \geq 0 \\ m_{ij} + \hat{I}_D & \text{for } m_{ij} < 0 \end{cases} \quad (21)$$

(cf. Fig.5(b)). As an analysis of the entire fundamental mains period shows, the control signals can then be closely approximated by

s'_R	s'_S	s'_T	$\varphi_N \in (-\frac{\pi}{3}, -\frac{\pi}{6})$	$\varphi_N \in (-\frac{\pi}{6}, 0)$
0	0	0	$(010)^-_{10}$	$(100)^+_{01}$
0	0	1	$(001)^-_{10}$	$(001)^-_{10}$
0	1	0	$(001)^+_{01}$	$(001)^+_{01}$
0	1	1	$(100)^+_{01}$ / $(010)^-_{10}$	$(100)^+_{01}$ / $(010)^-_{10}$
1	0	0	$(000)^0_{xx}$	$(000)^0_{xx}$
1	0	1	-	$(001)^-_{10}$
1	1	0	$(001)^+_{01}$	-
1	1	1	$(100)^+_{01}$	$(010)^-_{10}$

Tab.2: Relationship between the auxiliary switching function triple $(s'_R s'_S s'_T)$ and the actual switching states j in dependency on the polarity combinations of the line-to-line mains voltages and/or the angle φ_N. In the stationary case only the switching states $(100)^+_{01}$, $(010)^-_{10}$, $(001)^+_{01}$, $(000)^0_{xx}$ are required for $\varphi_N \in (-\frac{\pi}{3}, -\frac{\pi}{6})$, for $\varphi_N \in (-\frac{\pi}{6}, 0)$ only the switching states $(100)^+_{01}$, $(010)^-_{10}$, $(001)^-_{10}$, $(000)^0_{xx}$. The remaining auxiliary switching states (which appear only in the case of large reference values $\Delta i^*_{U,ij}$ are coded in such a way that the control error is reduced as fast as possible.

$$\begin{aligned} \frac{1}{\hat{I}_D}\tilde{m}_{RS} &\approx -M\cos(\varphi_N + \tfrac{\pi}{6}) &- m_0 \\ \frac{1}{\hat{I}_D}\tilde{m}_{ST} &\approx -M\sin(\varphi_N) &- m_0 \\ \frac{1}{\hat{I}_D}\tilde{m}_{TR} &\approx M\cos(\varphi_N - \tfrac{\pi}{6}) &- m_0 \end{aligned} \quad (22)$$

where

$$m_0 = \frac{3\sqrt{3}}{20} M \sin(3\varphi_N) \approx 0.26\, M \sin(3\varphi_N)\,. \quad (23)$$

This simplifies the practical realization.

3 Control Concept

The structure of a simple multi-loop control of the rectifier system is shown in **Fig.7**. By the pre-control signals m_{ij}, $ij = RS, ST, TR$, without explicite control input to the rectifier, input phase currents with a fundamental having the magnitude of the related mains phase current reference values $i^*_{N,i}$ are generated; furthermore, a symmetric magnetization of the transformer is guaranteed. The output $i^*_{C,i}$ of the capacitor phase voltage controllers $H(s)$ leads to an increase or decrease $\Delta i^*_{U,i}$ of the input phase currents $i_{U,i}$ and, accordingly, to a charging or discharging of the capacitors C. Finally, this brings the actual capacitor voltage values $u_{C,i}$ to the reference values $u^*_{C,i}$. One has to observe that according to Fig.2 $i_{U,i}$ is present always in two phases, i.e., the variation of one phase current influences one further phase current in any case. The coupling

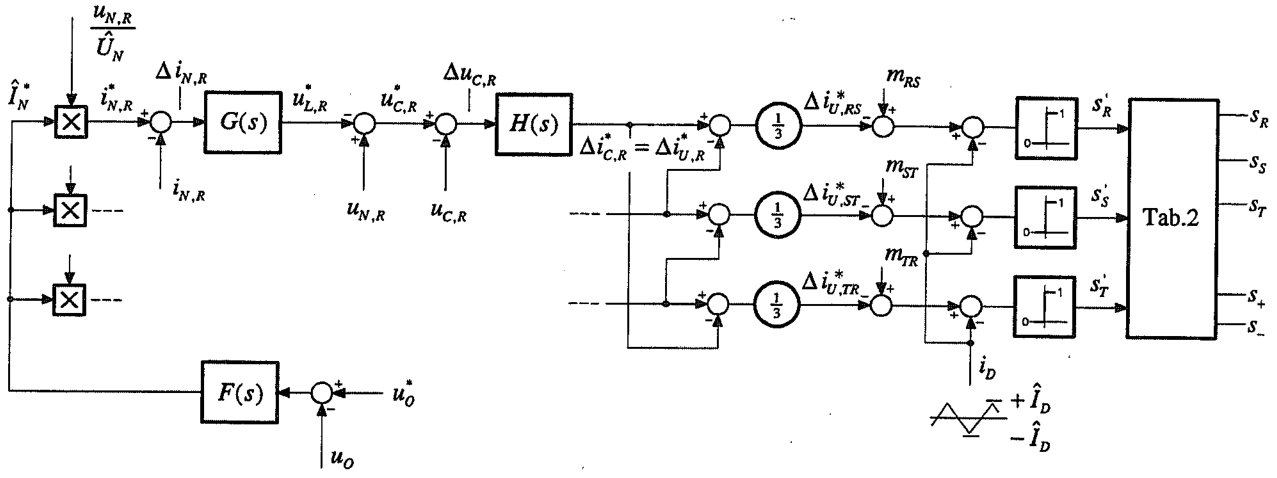

Fig.7: Structure of a 3-loop control (output voltage control loop, mains current control and input filter capacitor voltage control loop) of a VIENNA Rectifier III with pre-control m_{ij} of the mains current. The representation is partially only schematic for the sake of clearness. $\Delta i_{N,i} = i^*_{N,i} - i_{N,i}$ and $\Delta u_{C,i} = u^*_{C,i} - u_{C,i}$ denote the control errors of the mains phase currents and of the filter capacitor voltages, respectively.

of the phases has to be considered by transforming the reference values $\Delta i^*_{U,i}$ into line-to-line quantities

$$\begin{aligned} \Delta i^*_{U,RS} &= \frac{1}{3}(\Delta i^*_{U,R} - \Delta i^*_{U,S}) \\ \Delta i^*_{U,ST} &= \frac{1}{3}(\Delta i^*_{U,R} - \Delta i^*_{U,S}) \\ \Delta i^*_{U,TR} &= \frac{1}{3}(\Delta i^*_{U,T} - \Delta i^*_{U,R}) \end{aligned} \qquad (24)$$

[7]. Equation (24) guarantees that the system of the line-to-line currents formed thereby does not contain zero sequence quantities, i.e.,

$$\Delta i^*_{U,RS} + \Delta i^*_{U,ST} + \Delta i^*_{U,TR} = 0 \; . \qquad (25)$$

According to Fig.7 the reference value of the rectifier input current $i^*_{U,i}$ is gained by reducing the mains current reference value by the contribution $i^*_{C,i}$ required for forming the capacitor voltage. For the total reference value of the rectifier input current we have $i^*_{U,i} = i^*_{N,i} + \Delta i^*_{U,i}$. There, the mains current component $i^*_{N,i}$ is generated by the pre-control signals m_{ij}. $\Delta i^*_{U,i}$ is after transformation into line-to-line quantities subtracted from the pre-control signals. As shown in Fig.6 this yields a minor shift of the switching instants resulting from the pre-control in such a way that, finally, indeed (ideally) $i^*_{U,i}$ results as input current of the rectifier system.

The reference values $u^*_{C,i}$ of the filter capacitor voltages are given by superimposed mains phase current control loops $G(s)$. For guiding of the mains phase currents according to the reference values $i^*_{N,i}$, defined differential voltage fundamentals $u^*_{L,i}$ and/or capacitor voltages $u^*_{C,i} = u_{N,i} - u^*_{L,i}$ are required. Aiming for ohmic mains behavior, the mains current reference values $i^*_{N,i}$ are given in phase to the related mains phase voltages $u_{N,i}$; the amplitude $\hat{I}^*_N$ is set by the output voltage controller $F(s)$ in dependency of the power consumption of the load.

Remark: The transfer to line-to-line quantities could be made also already at the input of the capacitor voltage control. The reference values $u^*_{C,i}$ would have to be transformed into line-to-line quantities according to Eq.(24) and the line-to-line voltages could be used directly as actual values. In the case at hand the capacitor voltages are directly accessible if a star connection of the filter capacitors is applied; for a delta connection the star point has to be artificially formed separately. Furthermore, basically also an output voltage control with an inner output current control loop would be thinkable where the output current controller would have to set the reference values $u^*_{C,i}$ of the filter capacitor voltages on the primary. However, for this purpose no reference signals are available which can be derived directly from the mains phase voltages. This is opposed to the voltage proportional shape of the reference values of the mains phase currents (due to the resistive mains behavior) of the control according to Fig.7. Therefore, this control structure shall not be analyzed in more detail here.

4 Digital Simulation

Now the previous theoretical considerations shall be verified by digital simulation for, e.g., an application of the system as telecommunication power supply module (nominal output voltage 48V, rated power for three-phase input systems typical in the region 6...12kW) for the characteristic operating parameters

$$\begin{aligned} \hat{U}_{N,\mathrm{rms}} &= 327\,\mathrm{V} & \hat{I}^*_N &= 18\,\mathrm{A} \\ U_O &= 48\,\mathrm{V} & M &= 0.934 \\ f_P &= 20\,\mathrm{kHz} & \hat{I}_D &= 10\,\mathrm{A} \end{aligned}$$

(the switching frequency is selected relatively low in order to reduce the simulation time) and for the device parameters

$$\begin{aligned} L &= 0.5\,\mathrm{mH} \\ C &= 5\,\mu\mathrm{F} \\ L_O &= 1\,\mathrm{mH} \\ L_\mathrm{m} &= 5\,\mathrm{mH}\ . \end{aligned}$$

The modulation index of the pulse width modulation is set to $M = 0.934$; according to Eq.(15) we have then $\frac{N_1}{N_2} = 8.27$ and a primary current of $\frac{N_2}{N_1} I_O = 22.2\,\mathrm{A}$ appears (ripple neglected).

For the sake of limiting the consideration to the essentials, the output voltage will be assumed constant (impressed). Then, the power flow is defined directly by setting the amplitude $\hat{I}_N^*$ of the mains phase currents. Furthermore, the mains current control as well as the capacitor voltage control is performed applying simple P-type controllers

$$G(s) = \frac{u_{L,i}^*(s)}{\Delta i_{N,i}(s)} = 1.0\,\frac{\mathrm{V}}{\mathrm{A}} \tag{26}$$

and

$$H(s) = \frac{i_{C,i}^*(s)}{\Delta u_{C,i}(s)} = 0.1\,\frac{\mathrm{A}}{\mathrm{V}}\,, \tag{27}$$

with

$$u_{C,i}^* = u_{N,i} - u_{L,i}^*\,. \tag{28}$$

Due to the pre-control signals m_{ij} and $u_{N,i}$ the control errors remain limited in the stationary case to small values also without any I-type component of the controllers.

By the simulation results (shown in **Fig.8** and **Fig.9**) the applicability of the proposed control concept is demonstrated clearly. The mains current shows a largely sinusoidal shape, being in phase with the mains voltage. The voltage across the primary of the transformer is free of low-frequency spectral components; this becomes clear also by the shape of the magnetizing current i_m being symmetrical to 0 (cf. Fig.9).

4.1 Stresses on the Power Components

In order to simplify a comparison of the proposed circuit concept with alternate realizations, the current stresses on the power transistors as gained from simulation are compiled in the following:

$$\begin{aligned} I_{S,\mathrm{avg}} &= 5.8\,\mathrm{A} & I_{S,\mathrm{rms}} &= 11.2\,\mathrm{A} \\ I_{S+,\mathrm{avg}} &= 8.7\,\mathrm{A} & I_{S+,\mathrm{rms}} &= 13.8\,\mathrm{A} \\ I_{D_F,\mathrm{avg}} &= 2.9\,\mathrm{A} & I_{D_F,\mathrm{rms}} &= 7.9\,\mathrm{A} \\ I_{D_M,\mathrm{avg}} &= 2.9\,\mathrm{A} & I_{D_M,\mathrm{rms}} &= 8.0\,\mathrm{A} \\ I_{D_N,\mathrm{avg}} &= 5.8\,\mathrm{A} & I_{D_N,\mathrm{avg}} &= 11.2\,\mathrm{A}\ . \end{aligned} \tag{29}$$

It is interesting to note that these average and rms values can also be calculated directly analytically with very

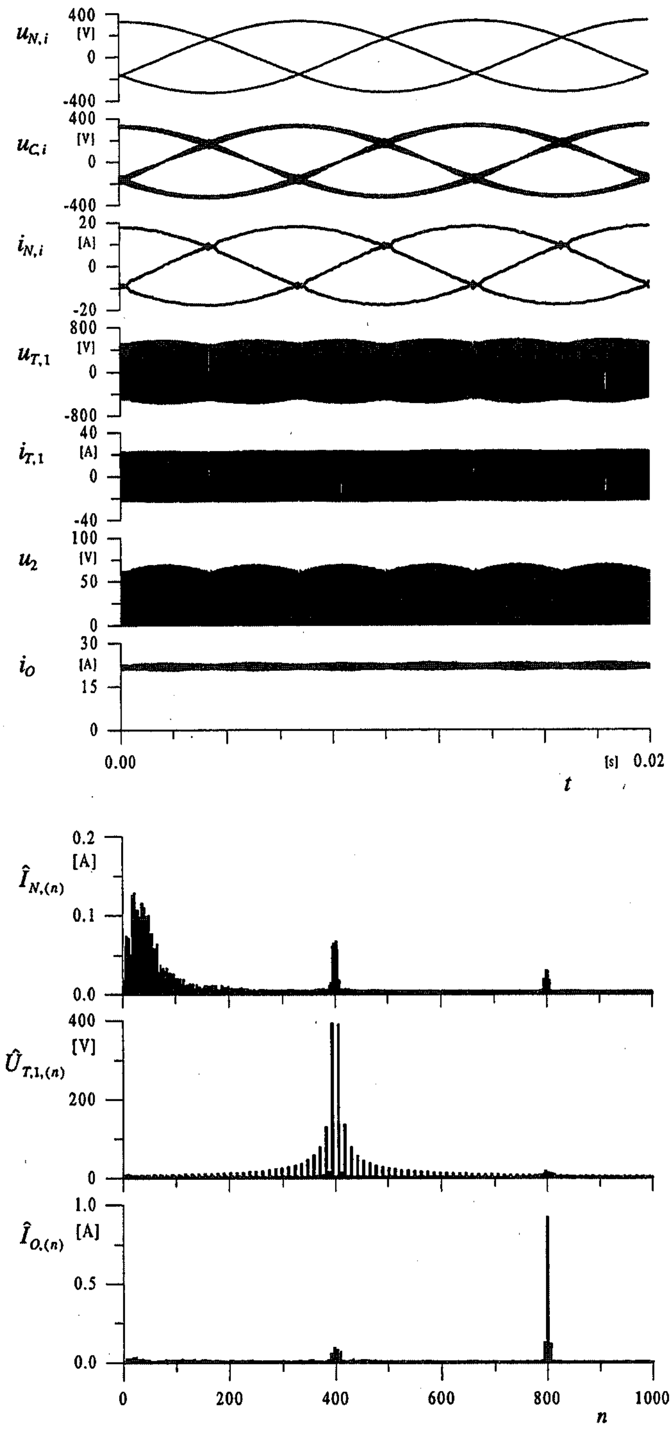

Fig.8: Digital simulation of the shape of the mains phase voltages $u_{N,i}$, the capacitor voltages $u_{C,i}$, the resulting mains currents $i_{N,i}$, the transformer primary voltage $u_{T,1}$, the transformer primary current $i_{T,1}$, the rectified transformer secondary voltage u_2 and the output current i_O. Further shown are the spectra of the mains currents (the fundamental component is suppressed), the transformer primary voltage and the output current (DC component suppressed). The transformer has been assumed ideal ($L_\sigma = 0$ and $L_\mathrm{m} \to \infty$). n denotes the order of the harmonics related to the mains frequency. Due to the rectification of $u_{T,2}$ the spectrum of u_2 shows significant harmonics only for frequencies being higher than twice the pulse frequency.

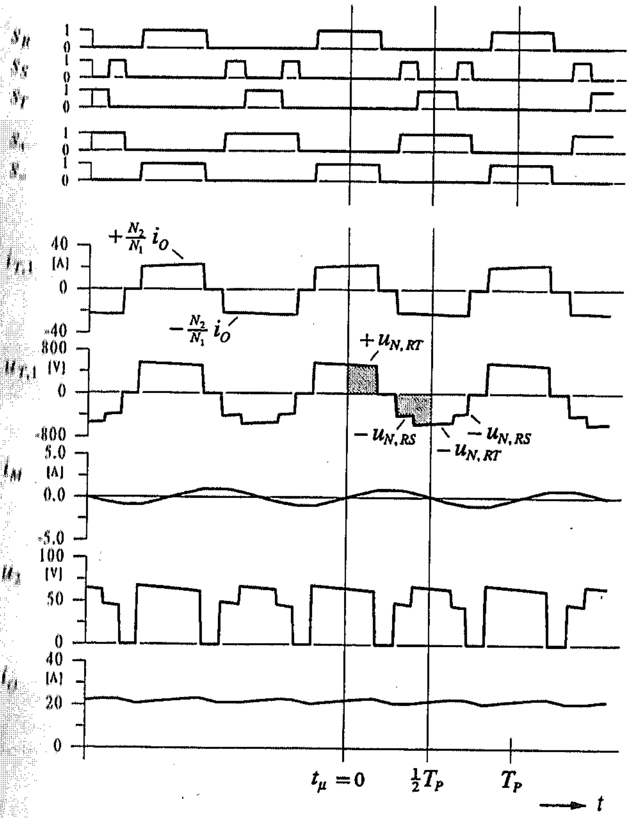

Fig.9: Digital simulation of the local shape of the control signals s_R, s_S, s_T, s_+, and s_-, of the transformer primary current $i_{T,1}$, transformer primary voltage $u_{T,1}$, magnetizing current i_m, rectified transformer secondary voltage u_2 and of the output current i_O for $\varphi_N \approx \frac{\pi}{12}$ and/or a switching state sequence $(100)^+_{01}$ - $(000)^0_{xx}$ - $(010)^-_{10}$ - $(001)^-_{10}$. According to the balance of positive and negative voltage-time areas of $u_{T,1}$ being present within a pulse period we get a purely AC pulse frequency magnetization of the transformer. Time scale: 25μs/div.

good precision in a simple way; this also shows clearly the functional dependency on the operational parameters. As described, e.g., in [16] for this purpose one has to replace the time-discontinuous valve currents by continuous equivalent currents i_{avg} and i_{eff} of equal local (related to a pulse period) average and/or rms values. E.g., there follows in $\varphi_N \in (-\frac{\pi}{6}, 0)$ for the current into the transistor S_R

$$
\begin{aligned}
i_{S_R,avg} &= \delta_{(100)^+_{01}} I_O \frac{N_2}{N_1} = \delta_{(100)^+_{01}} \frac{2}{\sqrt{3}} M^{-1} \hat{I}_N \\
i^2_{S_R,rms} &= \delta_{(100)^+_{01}} I_O^2 \frac{N_2^2}{N_1^2} = \delta_{(100)^+_{01}} \frac{4}{3} M^{-2} \hat{I}_N^2
\end{aligned} \quad (30)
$$

($\hat{I}_N \approx \hat{I}_N^*$). By averaging

$$
\begin{aligned}
I_{avg} &= \frac{1}{2\pi} \int_{2\pi} i_{avg} \, d\varphi_N \\
I^2_{rms} &= \frac{1}{2\pi} \int_{2\pi} i^2_{rms} \, d\varphi_N
\end{aligned} \quad (31)
$$

one finally receives the global rated current values related to a fundamental (mains) period; there, the averaging interval can also be reduced to $\frac{2\pi}{3}$ or $\frac{\pi}{2}$ under consideration of the periodicity and the symmetries of the shape of the quantity considered.

For the current stress on the transistors S_i and S_+ we have finally

$$
\begin{aligned}
I_{S_i,avg} &= \frac{1}{\pi} \hat{I}_N & I^2_{S_i,rms} &= \frac{2}{\sqrt{3}\pi} M^{-1} \hat{I}_N^2 \\
I_{S_+,avg} &= \frac{3}{2\pi} \hat{I}_N & I^2_{S_+,rms} &= \frac{\sqrt{3}}{\pi} M^{-1} \hat{I}_N^2
\end{aligned} \quad (32)
$$

(S_+ and S_- show equal current stresses). Then, the rated values of the diode current stresses can be calculated under consideration of the current distribution between the valves (e.g., there is always only a single diode $D_{F+,i}$ oder a single diode $D_{F-,i}$ conducting and/or only S_+ or S_- accepts the current) as follows

$$
\begin{aligned}
I_{D_F,avg} &= \frac{1}{3} I_{S_+,avg} = \frac{1}{2\pi} \hat{I}_N \\
I_{D_M,avg} &= \frac{1}{2} I_{S_i,avg} = \frac{1}{2\pi} \hat{I}_N \\
I_{D_N,avg} &= \frac{1}{\pi} \hat{I}_N
\end{aligned} \quad (33)
$$

and

$$
\begin{aligned}
I^2_{D_F,rms} &= \frac{1}{3} I^2_{S_+,rms} &&= \frac{1}{\sqrt{3}\pi} M^{-1} \hat{I}_N^2 \\
I^2_{D_M,rms} &= \frac{1}{6} I^2_{T_1,rms} &&= \frac{1}{\sqrt{3}\pi} M^{-1} \hat{I}_N^2 \\
I^2_{D_N,rms} &= \frac{1}{2} I^2_{S_i,rms} + I^2_{D_F,rms} &&= \frac{2}{\sqrt{3}\pi} M^{-1} \hat{I}_N^2 \; .
\end{aligned} \quad (34)
$$

Via similar considerations there follows for the rms value of the transformer primary current

$$
I^2_{T,1,rms} = 2 I^2_{S_+,rms} = \frac{2\sqrt{3}}{\pi} M^{-1} \hat{I}_N^2 \; . \quad (35)
$$

For the current stress on the input filter capacitors C one has in a first approximation

$$
I^2_{C,rms} = (\frac{4}{\sqrt{3}\pi} M^{-1} - \frac{1}{2}) \hat{I}_N^2 \; . \quad (36)
$$

5 Summary and Preview

In this paper a novel single stage PWM rectifier system based on the step-down principle with low effects on the mains is introduced and analyzed. It shows a substantial lower realization effort as compared to known circuit concepts with impressed output current (cf. Figs.1(a) and (c) in [5]). Therefore, the proposed system is of special interest for industrial applications. Furthermore, a substantial advantage lies in the possibility of a direct start-up without a previous charging of the output capacitor and/or the possibility of operating with impressed output current when the output is shorted. A disadvantage is given by the discontinuous shape of the input current making necessary a higher filtering effort for guaranteeing electromagnetic compatibility as compared to systems based on the boost-converter principle. Furthermore, the high frequency transformer is operated voltage-fed; this possibly implies the danger of saturating the magnetic core the transformer and/or the occurrence of overcurrents in case of load transients or for inexact generation of the firing/gating signals of the power transistors.

Therefore, the aim of further research is the analysis of the intrinsic stability of the magnetization due to the resistive components of the forward characteristics of the power semiconductors and the transformer primary. In a second step concepts for direct inclusion of the magnetization state of the transformer into an active symmetrization of the magnetic excitation are planned to be analyzed. There, the main issue is the isolated measurement of the magnetic flux density. Furthermore, guidelines for dimensioning of the system for a wide input and output voltage region shall be developed and the proposed circuit concept shall be compared with a two-stage solution [9] concerning efficiency and realization effort. Based on these results, the advantageous operating regions of the VIENNA Rectifier III shall be determined.

References

[1] **Manias, S., and Ziogas, P.D.:** *A Novel Sinewave in AC to DC Converter with High-Frequency Transformer Isolation.* IEEE Transactions on Industrial Electronics, Vol. IE-32, No. 4, pp. 430–438 (1985).

[2] **Wang, K., Lee, F.C., Borojevic, D., and Yan, X.:** *A New Quasi-Single-Stage Isolated Three-Phase ZVZCS Buck PWM Rectifier.* Record of the 27th IEEE Power Electronics Specialists Conference, Baveno, Italy, June 23–27, Vol. 1, pp. 449-455 (1996).

[3] **Kolar, J.W., Ertl, H., and Zach, F.C.:** *Realization Considerations for Unidirectional Three-Phase PWM Rectifier Systems with Low Effects on the Mains.* Proceedings of the 6th International Conference on Power Electronics and Motion Control, Budapest, Oct. 1–3, Vol. 2, pp. 560–565 (1990).

[4] **Malesani, L., and Tenti, P.:** *Three-Phase AC/DC PWM Converter with Sinusoidal AC Currents and Minimum Filter Requirements.* IEEE Transactions on Industry Applications, Vol. IA-23, No. 1, pp. 71–77 (1987).

[5] **Kolar, J.W., Drofenik, U., and Zach, F.C.:** *VIENNA Rectifier II - A Novel Single-Stage High-Frequency Isolated Three-Phase PWM Rectifier System.* Proceedings of the 13th IEEE Applied Power Electronics Conference, Anaheim (CA), Feb. 15–19, Vol. 1, pp. 23–33 (1998).

[6] **Koczara, W.:** *Unity Power Factor Three-Phase Rectifier.* Proceedings of the 6th International (2nd European) Power Quality Conference, Munich, Germany, Oct. 14–15, pp. 79–88 (1992).

[7] **Nishida, Y., Maeda, A., and Tomita, H.:** *A New Instantaneous-Current Controller for the Three-Phase Buck-Boost and Buck Converters with PFC Operation.* Proceedings of the 10th IEEE Applied Power Electronics Conference, Dallas (TX), March 5–9, Vol. 2, pp. 875–883 (1995).

[8] **Itoh, S., and Fukuda, S.:** *Basic Considerations of Active Power Filter using Current Source Converter.* Proceedings of the 1st International Power Conversion Conference, Tokyo, Dec. 8–10, pp. 443–452 (1995).

[9] **Ide, P., Froehleke, N., and Grotstollen, H.:** *Comparison of Selected 3-Phase Switched Mode Rectifiers.* Proceedings of the 19th International Telecommunications Energy Conference, Melbourne, Oct. 19–23, pp. 630–636 (1997).

[10] **Apeldoorn, O., Skullerud, T., De Doncker, R., and Undeland, T.:** *Minimizing the Line Interference of High-Power Low-Frequency Converters.* Proceedings of the 7th European Conference on Power Electronics and Applications, Trondheim, Sept. 8–10, Vol. 3, S. 250–255 (1997).

[11] **Nishida, Y., and Maeda, A.:** *A Simplified Discontinuous-Switching-Modulation for Three-Phase Current-Fed PFC-Converters and Experimental Study for the Effects.* Proceedings of the 11th IEEE Applied Power Electronics Conference, San Jose (CA), March 3–7, Vol. 2, pp. 552–558 (1996).

[12] **Espinoza, J., Joos, G., and Ziogas, P. D.:** *An Integrated Three-Phase Voltage Regulated Current Source Inverter Topology.* Proceedings of the IEEE International Symposium on Industrial Electronics, Budapest, June 1–3, pp. 663–668 (1993).

[13] **Espinoza, J., and Joos, G.:** *On-Line Generation of Gating Signals for Current Source Converter Topologies.* Proceedings of the IEEE International Symposium on Industrial Electronics, Budapest, June 1–3, pp. 674–678 (1993).

[14] **Zargari, N. R., Joos, G., and Ziogas, P. D.:** *Input Filter Design for PWM Current-Source Rectifiers.* Proceedings of the 8th IEEE Applied Power Electronics Conference, San Diego (CA), March 7–11, pp. 824–830 (1993).

[15] **Fukuda, S., and Yamaji, M.:** *Design and Characteristics of Active Power Filter using Current Source Converter.* Conference Record of the 25th IEEE Industry Applications Society Annual Meeting, Seattle, Oct. 7–12, Pt. II, pp. 965–970 (1990)

[16] **Kolar, J.W., Ertl, H., and Zach, F.C.:** *Calculation of the Passive and Active Component Stress of Three-Phase PWM Converter Systems with High Pulse Rate.* Proceedings of the 3rd European Conference on Power Electronics and Applications, Aachen, Germany, Oct. 9–12, Vol. 3, pp. 1303–1311 (1989).

[17] **Bose, B.K.:** *Recent Advances in Power Electronics.* IEEE Transactions on Power Electronics, Vol.7, No.1, pp. 2–16 (1992).

[18] **Mohan, N., Undeland, T.M., and Robbins, W.P.:** *Power Electronics: Converters, Application and Design,* 2nd Edition, New York: John Wiley & Sons (1995).

NORPIE/98

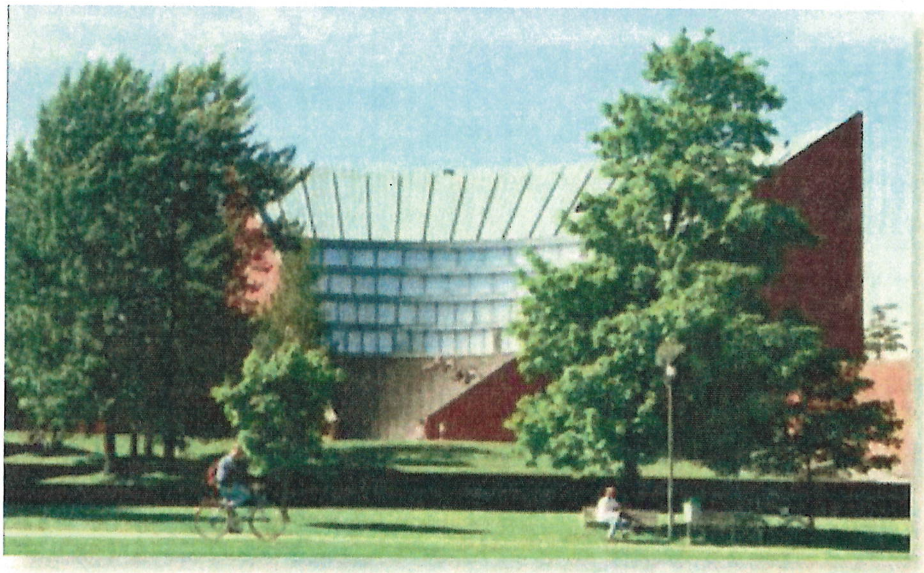

1998 IEEE Nordic Workshop on Power and Industrial Electronics

Helsinki University of Technology
August 26–27, 1998

Workshop Proceedings

pels